Model-based framework for multidisciplinary optimisation of early-stage aircraft wing design

G. Pagliuca
g.pagliuca@cranfield.ac.uk

Research Fellow - RAeS Associate Member
School of Aerospace, Transport and Manufacturing
Cranfield University
United Kingdom

T. Kipouros
t.kipouros@cranfield.ac.uk

Lecturer in Computational Engineering Design Optimisation - RAeS Member
School of Aerospace, Transport and Manufacturing
Cranfield University
United Kingdom

A. M. Savill
mark.savill@cranfield.ac.uk

Professor of Computational Aerodynamics Design - RAeS Fellow
School of Aerospace, Transport and Manufacturing
Cranfield University
United Kingdom

ABSTRACT

Multidisciplinary optimisation aims to enhance aircraft design by identifying the most promising configurations at early-stage. The approach proposed in this paper exploits model-based engineering principles for the development of a versatile software framework which can include multiple disciplines with multiple fidelity levels. A wing planform optimisation procedure for transonic aircraft is established by focusing on minimum drag coefficient, maximum aerodynamic efficiency and minimum operating empty weight. Three models are employed, specifically for aircraft mass estimation, longitudinal stability and aerodynamics. The latter computes aircraft aerodynamic performance using corrected Vortex Lattice Method and either Radial Basis Function interpolation or Neural Network as surrogate models to speed-up the process. Results are provided for the multi-objective optimisation of the wing planform of the Common Research Model. In addition, the impact of surrogate modelling for aerodynamics on early-stage design is investigated and an effective strategy to minimise computational time is proposed as framework's feature. Overall, the framework allows for a quick identification of optimal wing planforms and it provides effective guidance to the human designer.

Acronyms

CAD Computer Aided Design
CRM Common Research Model
OEW Operating Empty Weight
PSO Particle Swarm Optimisation
RBF Radial Basis Function
TPS Thin Plate Spline
VLM Vortex Lattice Method

1.0 Introduction

Multidisciplinary optimisation represents the new frontier of aircraft design [1]. It promises to reduce cost and time for developing new products by providing better configurations at an earlier stage [1, 2]. In this context, gradient-free optimisation techniques, which do not rely on differentiable objective functions, are often adopted by engineers to optimise complex systems [3]. They proved to be an effective choice when a large number of design variables are involved [4] and this is the case of early-design since no decision about the aircraft configuration is made at that stage. Usually, gradient-free methods require many evaluations of the objective function and this can lead to high computational cost. However, such cost ultimately depends on simulations' accuracy and multi-fidelity approaches have been proposed in literature as a remedy for shape optimisation [5, 6]. A multi-fidelity application of aerodynamic optimisation to early-design for general aviation aircraft is proposed in [7]. A genetic algorithm is exploited to identify the best propeller locations. Aerodynamics is modelled with both computational fluid dynamics and low-fidelity tools. Another strategy often employed for multi-fidelity applications is surrogate modelling which speeds-up the optimisation process by exploiting a database of pre-computed data [5, 6].

Including additional disciplines besides aerodynamics needs the development of a multidisciplinary framework for optimisation purposes. A summary of possible strategies targeting high-fidelity simulations is presented in [8]. The distinction is made between monolithic and distributed architectures while it is highlighted that further research is needed on the latter. Another example of framework is given in [9] where a genetic algorithm is adopted to optimise general aviation aircraft at conceptual design stage. The optimisation is performed using software units corresponding to distinct disciplines and it is led by airworthiness requirements. Generally, applications found in the academic literature provide only a small number of tools to calculate aerodynamic and structural performance. However, early-stage design in the industrial context requires a framework capable of incorporating existing tools and database of experimental data in order to give complete freedom to the designer [10].

A possible solution to address this problem as well as including multi-fidelity is to implement a software framework according to model-based engineering principles [11]. Such frameworks rely on a set of distinct models with definitions of how they interact [11]. Although model-based principles have been available in literature since the beginning of 90s, their application to aircraft design is a recent development. In [10] a model-based framework is employed to study the performance of general aviation aircraft. Besides aerodynamics, the system includes models for physical parts such as engines and fuel tanks among others. The resulting framework is versatile since it incorporates existing tools developed in a variety of

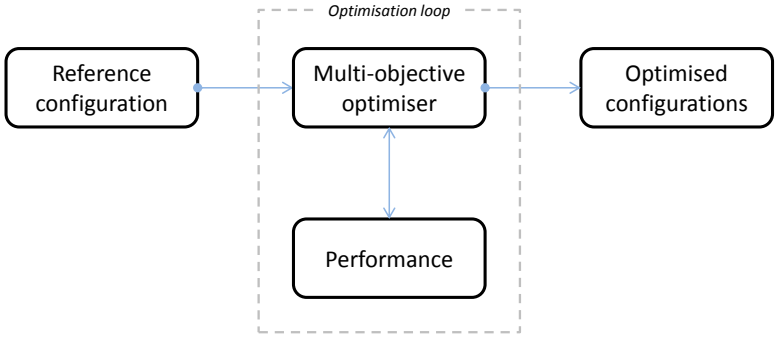

Figure 1. Workflow for the optimisation loop.

programming languages as well as models based on experimental data. In addition, information is encapsulated inside models so that data-transfer is minimised during simulations. This improves the overall computational cost and allows large scale simulations composed of many interacting software components.

In this paper, a model-based approach is exploited for multidisciplinary optimisation of wing planform for transonic aircraft at early-stage design. The aim is to provide the designer with a useful tool which is able to take into account targets and constraints coming from multiple disciplines and suggest modifications to the reference geometry. The paper proceeds with a description of the framework in Section 2. The wing planform optimisation problem is formulated in Section 3. Results are given in Section 4 for the particular case of optimising the Common Research Model (CRM) wing. The model-based framework allowed for an investigation concerning surrogate modelling for aerodynamics and results are given in the second part of Section 4. Conclusions and an outlook of future work are given in Section 5.

2.0 Method

The optimisation loop is implemented using a model-based approach [11] with parametrisation of the model, objective functions and constraints defined by the user. Specifically, the implementation is coded in an object-oriented way [12]. Interfaces declare inputs and outputs capabilities for each distinct class of models. In turns, a model belonging to a given class must meet the requirements set by the interface. Communication between models is only allowed through channels defined by interfaces. As a result, the software is composed of models and definitions of their interactions. In turn, each model can use one or more tools to undertake its task so that multi-fidelity approaches and reusing of existing data and software are possible.

The workflow for the optimisation is depicted in Fig. 1 where the interconnections between models are highlighted. The model-based architecture requires that each block in Fig. 1 is composed of an interface and an associated model. Regarding the optimiser, it is based on Particle Swarm Optimisation (PSO) algorithm implemented in parallel [13]. It performs a search for global optimality which requires up to thousands evaluations of the objective function. The objective function depends on the parametrisation defined by the user and it can be a weighted sum of single objectives. The optimiser interrogates the performance model to compute the objective function and assess new sets of parameters. Optimal solutions are returned when the maximum number of iterations is reached or a convergence criterion is met.

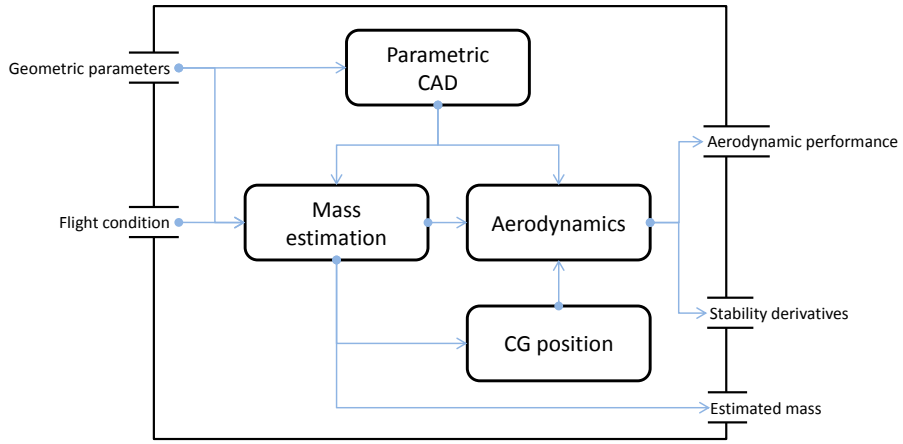

Figure 2. Graphical representation of the performance model.

Regarding the performance model, it is intended for the purpose of wing planform optimisation and its layout is shown in Fig. 2 with inputs and outputs placed on the left and right sides of the block, respectively. The user defines a flight condition and a wing planform to be assessed. The flow of the information is clearly identifiable and four other models concerning geometry, aerodynamics, mass estimation and centre of gravity are involved. Starting from geometric parameters given as input by the optimiser, a new geometry is produced by the parametric Computer-Aided Design (CAD) model. The mass estimation model provides a value for the aircraft mass and its spacial distribution. The centre of gravity position is calculated using such mass distribution by a model developed on purpose. The flight condition is then used by the aerodynamic model to compute lift and moment which guarantee equilibrium of forces. The model provides angle-of-attack, tail rotation, load distribution and stability derivatives. Output is collected from all these models and made available to the optimiser for the next iteration.

A brief description of models composing the performance block is provided hereafter. The parametric CAD used by the geometry model is an in-house code developed at Airbus for the purpose of early-stage design. Parametrisation concerns wing planform but it is not limited to geometrical quantities in general. Mass estimation is performed with semi-empirical methods discussed in [14] and implemented in the corresponding model. The operating empty weight (OEW) is computed by referring to a target maximum take-off weight. Contributions from fuselage, wing, horizontal and vertical tails, landing gear, engines are taken into account. Additional weight to cope with buckling and critical load factors is considered. Centre of gravity position is obtained from the mass distribution. Such information is needed to compute stability derivatives accurately. The implementation of the aerodynamic model follows a multi-fidelity paradigm using multiple tools with fidelity levels ranging from empirical theories for finite wings [15] to vortex lattice method (VLM) [16]. Three tools are exploited in this paper. The first is the open-source VLM code AVL [17]. A trim calculation is performed so that angle-of-attack and horizontal tail deflection are updated to meet lift and moment requirements. When transonic flows are involved, results from AVL are corrected with empirical methods so that wake and viscous contributions are added to the drag coefficient. Stability derivatives are computed with finite differences around the trimmed solution

and taking the centre of gravity as reference point. Secondly, a surrogate model based on radial basis function interpolation (RBF) [18, 19] is available. A database of aerodynamic data, which can contain either experimental or pre-computed data, is employed to interpolate the aerodynamic performance for new configurations. Thirdly, an artificial neural network [20] based on multilayer perceptron algorithm [21] and a logistic activation function is an additional surrogate for the aerodynamic model. One hidden layer is adopted and its number of neurons is obtained by tuning the network to the specific test case. Weights for the neurons are computed with back-propagation [22]. The implementation relies on an open-source machine learning framework implemented in Python [23].

3.0 Formulation

The wing planform optimisation problem is formulated in this section. A typical transonic wing is unequivocally defined with seven parameters as shown in Fig. 3(a). The sequence of parameters is named configuration. They represent displacements from the wing planform to be optimised. Thus, when all the parameters are zero, the baseline wing is obtained. Precisely, parameters P1, P2, P3 define the vertical displacement of the trailing edge points with P1 defining the root chord. Note that the first, straight, part of the wing in Fig. 3(a) is assumed to be inside the fuselage and its spanwise length is assumed to be constant. Parameters P4 and P5 define the leading edge location so that chord lengths at the kink and at the tip are given by P5 - P2 and P4 - P3, respectively. Apart from the root chord P1 for which a maximum variation of $\pm 10\%$ from the reference is allowed, the parameters are not bounded. The set of geometrical constraints are reported in Fig. 3(b). They mainly avoid planforms with negative sweep angles or M-shaped wings by requiring a positive clockwise angle between the three segments which define each edge. In addition, a minimum length constraint $c_{\min}$ is imposed on the tip chord to avoid pointy wings. Besides geometrical constraints, a requirement for a stable configuration is formulated. The corresponding inequality is based on the value of the $\mathrm{d}C_m/\mathrm{d}\alpha$ stability derivative which must be negative for longitudinally stable aircraft. When using VLM aerodynamics, configurations with angle-of-attack and elevator angles outside the range $[-4, 4]$ were considered not physical and discarded. Overall, the parametrisation allows the planform to assume a variety of shapes ranging from rectangular straight to tapered swept wings.

Regarding the objective function, it can be chosen among OEW, aerodynamic efficiency and drag coefficient. Its value is referred to the performance of the baseline geometry according to the practice usually adopted in early-stage aircraft design. The mathematical formulation of the problem is summarised in Table 1.

4.0 Results

The model-based software architecture was exploited to optimise the wing planform of the Common Research Model (CRM) [24] flying at Mach number $M = 0.85$, altitude of 10000m, take-off weight of 2.472×10^5 kg. The baseline geometry is illustrated in Fig. 4 using the parametric CAD. It is composed of wing, fuselage, horizontal tail and the latter can be rotated around its mid-chord axis. The geometry of the torsion box, size and distribution of ribs are defined parametrically depending on wing geometry.

The optimisation is performed applying PSO and successful convergence is assumed when the maximum distance between positions of swarm particles and the swarm best particle is

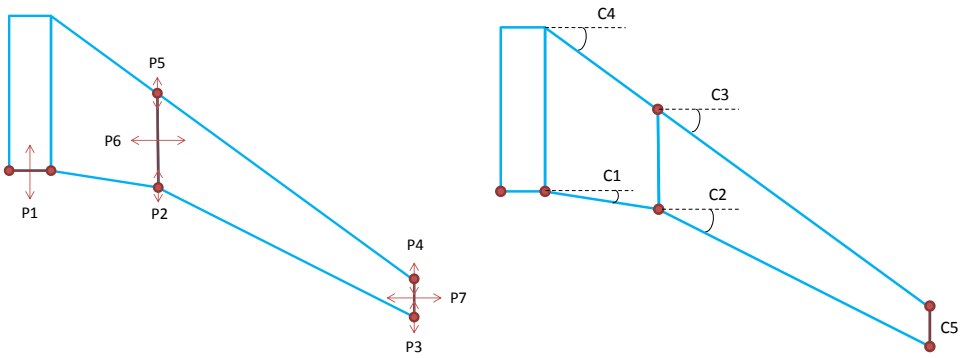

(a) Parameters (b) Constraints

Figure 3. Geometric parameters and constraints used for the optimisation.

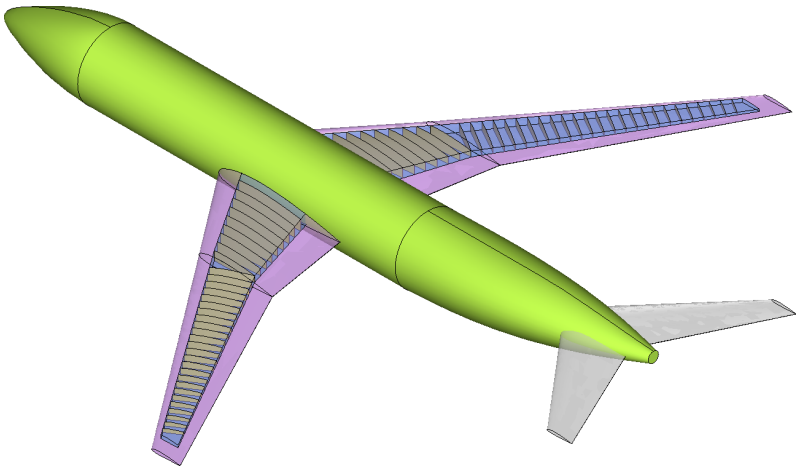

Figure 4. Baseline geometry of the CRM as depicted with the parametric CAD software.

smaller than 1×10^{-5} at two successive iterations. Velocity is updated for each particle every iteration by taking into account 50% of its velocity at the previous iteration, 50% of particle's change of position and 50% of swarm best particle's velocity. Simulations can be performed either in serial or parallel with an implicit-parallelism paradigm.

Optimisation was first performed using VLM with empirical corrections for transonic flows as a tool for the aerodynamic model. The acronym VLM will be used in the following to refer to this model. Three single-objective optimisations were performed, specifically maximising aerodynamic efficiency, minimising OEW and drag coefficient. The PSO optimiser was run with a swarm size of 128 and maximum number of iterations was set to 10. Results are presented with wing planform and lift distribution in Fig. 5 and they are compared to reference values computed for the CRM baseline. Results minimising single-objectives correspond to impractical configurations since not all requirements of the problem are taken into account. For example, the wing planform maximising aerodynamic efficiency is shown in Fig. 5(a). Wingspan is larger and overall the wing is more slender when compared to the underlying

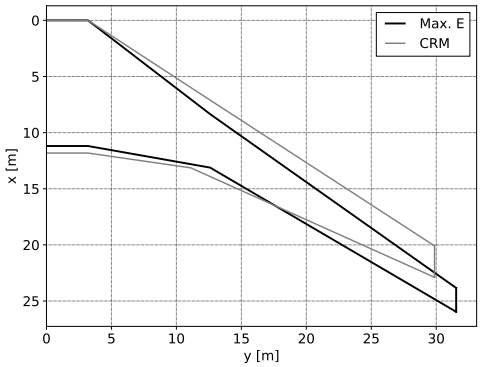

(a) Wing planform for maximum aerodynamic efficiency

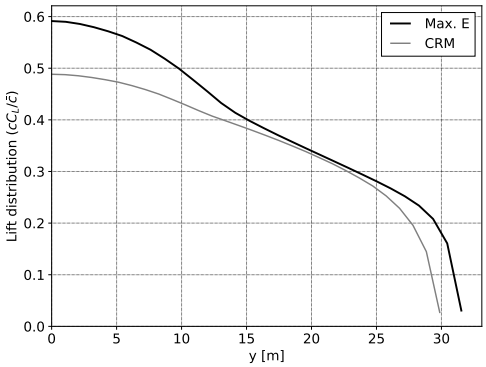

(b) Lift distribution for configuration providing maximum aerodynamic efficiency

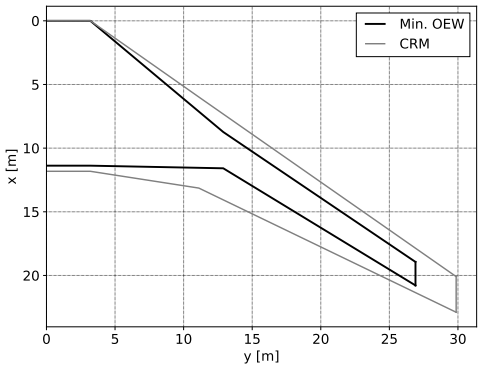

(c) Wing planform for minimum OEW

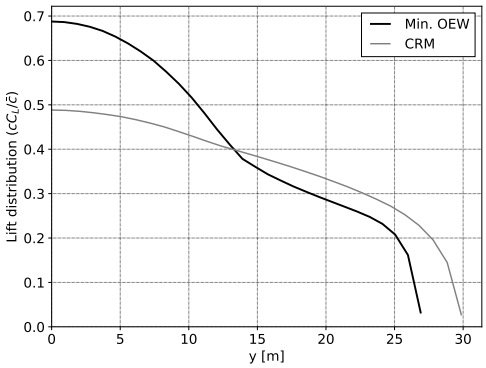

(d) Lift distribution for configuration providing minimum OEW

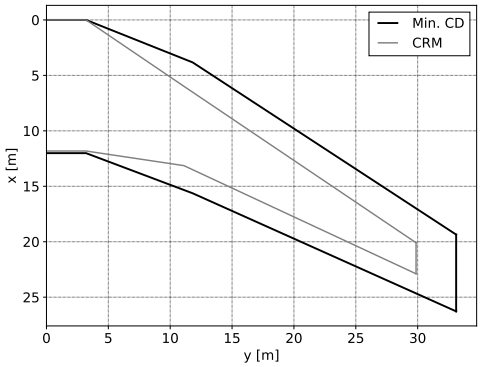

(e) Wing planform for minimum drag coefficient

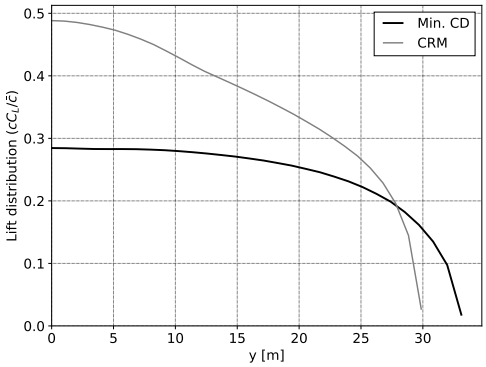

(f) Lift distribution for configuration providing minimum drag coefficient

Figure 5. Selected configurations produced by the optimiser.

	Function/Variable	Description
minimise	$f \in \left\{ \frac{CD}{CD_{\text{ref}}}, \frac{OEW}{OEW_{\text{ref}}}, -\frac{E}{E_{\text{ref}}} \right\}$	Objective function chosen from a set of design targets
with respect to	$P_i \quad \forall i \in [1, 7]$	Wing platform alterations with respect to the baseline
subject to	$c_3 \geq c_4 \geq 0$ $c_2 \geq c_1 \geq 0$ $c_5 \geq c_{\text{min}}$	Geometric constraints to limit the optimisation to wings with positive sweep angle and a minimum chord length at the tip
subject to	$\frac{\mathrm{d}C_m}{\mathrm{d}\alpha} < 0$	Condition for a statically stable aircraft

Table 1. Formulation of the multidisciplinary optimisation problem.

reference. The corresponding lift distribution is in Fig. 5(b). The total C_L is larger than the reference value and most of the increment in the loading is located at the wing root. Aerodynamic efficiency is improved by 7.8%, OEW decreased by 1.2% and drag coefficient increased by 8.6%. The configuration shown in Fig. 5(c) minimises the OEW by concentrating most of the mass close to the wing root. The outer part of the wing is very slender and the wingspan reduced. The structural mass required by such wing is 6% smaller than the one needed by the baseline geometry. The plot in Fig. 5(d) shows that most of the load is carried by the inner part of the wing. Aerodynamic efficiency is reduced by 7.8% and drag coefficient increased by 61%. In Fig. 5(e), the planform with minimal drag coefficient is depicted. The resulting planform has a small taper ratio with a positive sweep angle to reduce the shock drag coefficient. Induced drag coefficient is minimised with a larger wingspan. The lift distribution, which is shown in Fig. 5(f), has an almost monotonic decrease when starting from the root chord. Drag coefficient is reduced by 28% but OEW is increased by 14%. Although the configurations in Figs. 5(a), 5(c) 5(e) are interesting from the academic point-of-view, they are impractical for industrial designers since they focus on a single objective at once. Multiple, conflicting objectives must be taken into account during the optimisation.

Two-objective optimisation

Focus is now on configurations which are a trade-off of two objectives. Optimisations were performed using PSO with a swarm size of 128 for 48 iterations. Specifically, three optimisations are considered. The first one minimises OEW and maximises aerodynamic efficiency and the outcome is presented in Fig. 6. Configuration A is chosen as optimal solution located on the Pareto front as shown in Fig. 6(a). The wing planform is shown in Fig. 6(b) where it is compared to the baseline. OEW is minimised by 3.7% with a reduction of wingspan. The

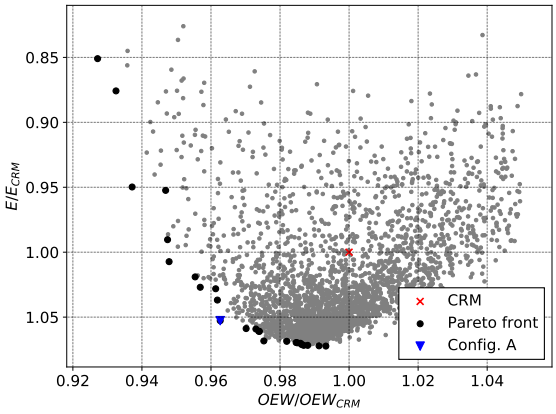

(a) Pareto front for OEW and aerodynamic efficiency

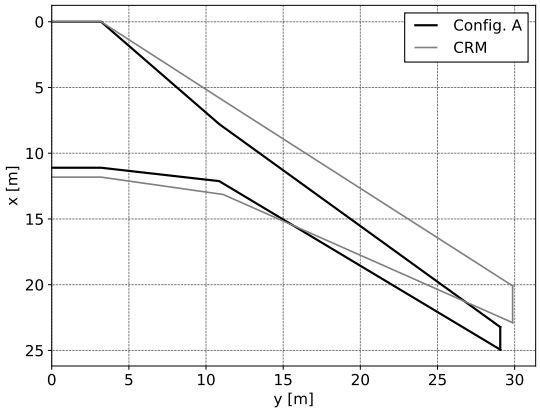

(b) Wing planform

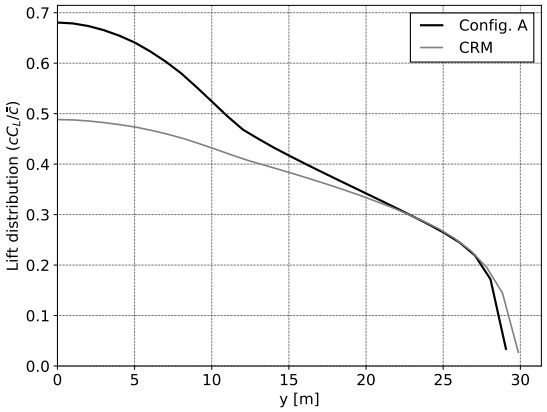

(c) Lift distribution

Figure 6. Results for configuration A which is on the Pareto front obtained by minimising OEW and maximising aerodynamic efficiency.

kink moves outward so that the trailing edge sweep angle of the inner wing is reduced. Overall, the wing is more slender and this factor improves aerodynamic efficiency by 5.2%. The quarter-chord sweep angle is larger when compared to the baseline. Lift distribution is given in Fig. 6(c) for the same configuration. In general, wing loading is increased everywhere and drag coefficient, which is not included in the optimisation, increases by 30%.

Regarding the second optimisation in Fig. 7, it minimises both OEW and drag coefficient. Configuration B is located on the resulting Pareto front as depicted in Fig. 7(a). Its wing planform is very similar to the CRM baseline, Fig. 7(b). The kink is slightly moved outward while few changes were found for sweep angle. In particular, trailing edge sweep angle does not change significantly. Overall, the lift distribution in Fig. 7(c) is smooth and lower everywhere. Results for configuration B suggest a consideration. Little modifications to the baseline improve both drag coefficient and OEW by 2.5% and 1%, respectively, while aerodynamic efficiency decreases by only 0.25%. The optimiser managed to identify these key modifications without relying on human experience. The educational implications are clear since this tool could help inexperienced engineers to improve their designs.

A third optimisation was performed which maximises aerodynamic efficiency and minimises drag coefficient and its results are reported in Fig. 8. Configuration C is an one optimal solution on the Pareto front which is shown in Fig. 8(a). The wing planform depicted in Fig. 8(b) is very slender. The wingspan is increased by more than 5 meters while the tip chord is kept at the minimum. The root chord is slightly reduced and the kink is moved outward. Sweep angle for the inner wing decreases whereas it is unaltered for the outer part. Lift distribution is shown in Fig. 8(c) and compared to corresponding results for the baseline. Load is smaller everywhere along the wingspan. Additional lift is produced by the outer part of the wing. Thus, aerodynamic efficiency increases by 4.5% and drag coefficient is reduced by 7.3%. However, OEW is not taken into account and it increases by 2%.

Multi-objective optimisation

Multi-objective optimisation was performed for three objectives simultaneously. Specifically, OEW and drag coefficient are minimised while aerodynamic efficiency is maximised. Particle swarm optimiser was run with a swarm size of 128 for 48 iterations. The resulting three-dimensional Pareto front is shown in Fig. 9(a). Identifying the reference configuration for CRM in the plot is quite difficult. It is dominated and, thus, located in the cloud of points. A configuration named D is chosen on the Pareto front and depicted in Fig. 9(b). Regarding the inner wing, its sweep angle is smaller than the reference's one. Conversely, the outer wing shows an slightly increased sweep angle. Overall, the wing span increases by 10%, the wing kink moves outward and the tip chord is slightly smaller as well. The corresponding lift distribution is shown in Fig. 9(c). Load increases on the inner wing but it is almost identical to the reference from the kink onward. Lift distribution is extended because of the longer wing span and this results in a higher global lift coefficient for the wing. Aerodynamic efficiency is increased by 5.6%, drag coefficient reduced by 4.1% and OEW decreased by 0.8%. The multi-objective optimisation implemented inside the model-based framework proved to be an effective tool to improve multidisciplinary objectives simultaneously.

4.1 Surrogate modelling for aerodynamics

The model-based framework allows for substitution of models at any time. This feature was exploited to replace the aerodynamic model based on VLM and an investigation on surrogate

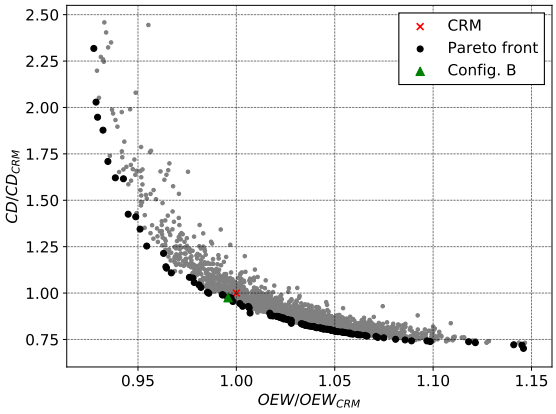

(a) Pareto front for OEW and drag coefficient

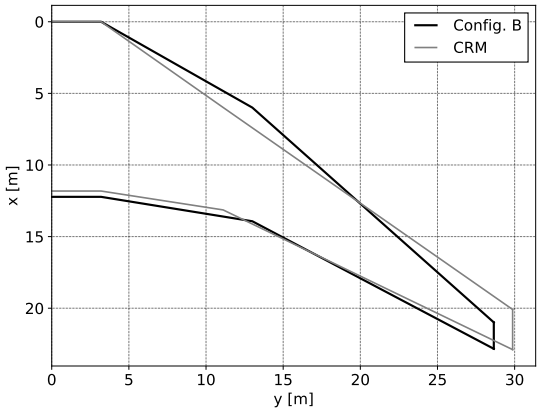

(b) Wing planform

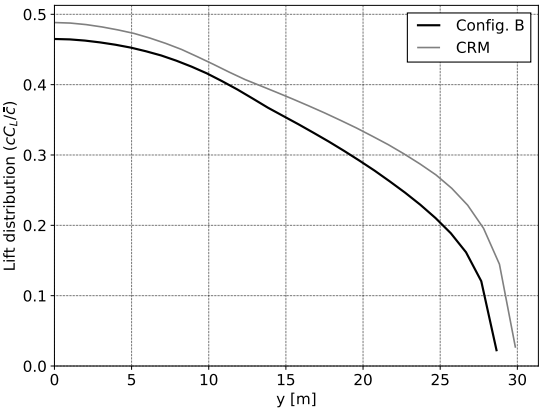

(c) Lift distribution

Figure 7. Results for configuration B which is on the Pareto front obtained by minimising both OEW and drag coefficient.

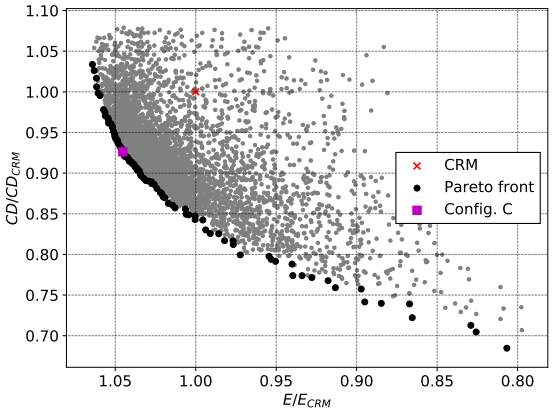

(a) Pareto front for aerodynamic efficiency and drag coefficient

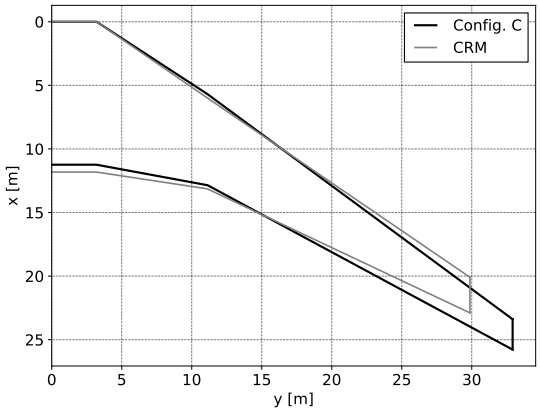

(b) Wing planform

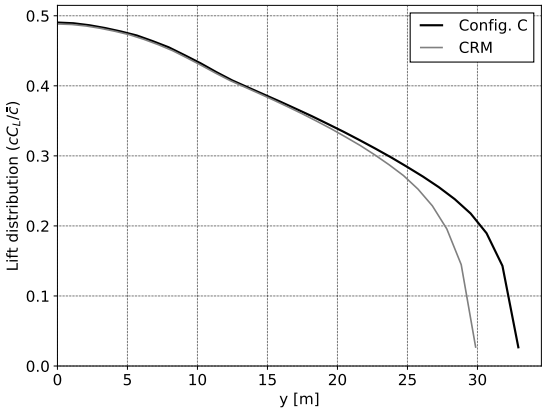

(c) Lift distribution

Figure 8. Results for configuration C which is on the Pareto front obtained by maximising aerodynamic efficiency and minimising drag coefficient.

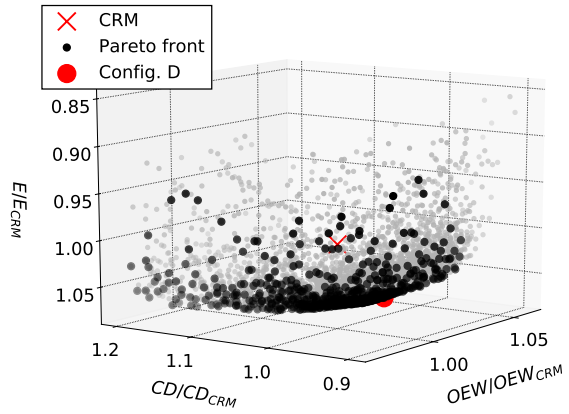

(a) Three-objective Pareto front

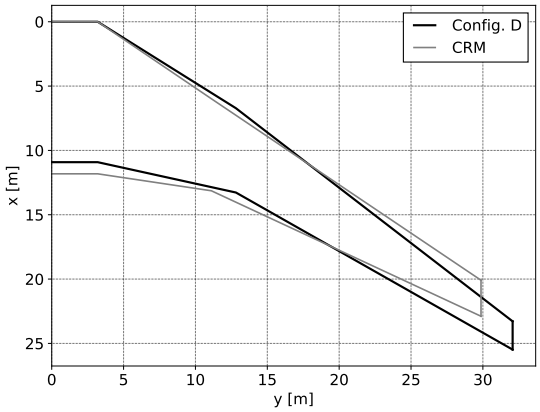

(b) Wing planform

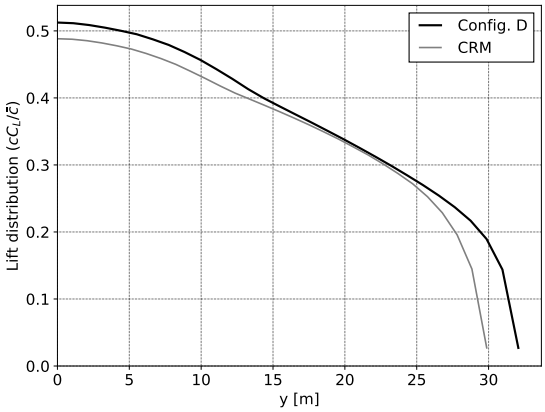

(c) Lift distribution

Figure 9. Results for configuration D which is on the Pareto front obtained by maximising aerodynamic efficiency, minimising drag coefficient and minimising OEW.

modelling is presented in this section. The main challenge is the variety of wing planforms which need to be assessed. Their geometries can differ considerably and surrogate models should be able to provide accurate results with a limited set of data. Two types of surrogate models were investigated, specifically RBF interpolation and neural network. They both rely on a database of pre-computed aerodynamic data to evaluate performance of new configurations. Inputs consist in the seven geometrical parameters which define the wing planform. Outputs are 8 and they include lift coefficient, angle-of-attack, drag coefficient and aerodynamic efficiency. Without loss of generality, performance of surrogate models is compared to VLM aerodynamics by reporting results for a two-objective optimisation which aims to minimise both OEW and drag coefficient. Similar results were obtained for optimisation aiming to maximise aerodynamic efficiency and minimise either OEW or drag coefficient but they are not reported in the paper for sake of brevity. A quantification of the error provided by surrogate models is obtained by recomputing optimal configurations with VLM. Specifically, a VLM computation is performed for each configuration on the Pareto front and values of objective functions are compared to the ones provided by the surrogate model. Their ratios with respect to exact values provided by VLM are collected so that average error and standard deviation are computed and expressed as a percentage.

Regarding the aerodynamic database, it can be populated with pre-existing experimental data when it is available. For this paper, it will be generated using VLM instead. The 7 parameters which define the wing planform (Tab. 1) are now limited to the range $p_i \in [-4, 4], \forall i \in [2, 6]$. An exception is made for the root chord which spans a smaller range $p_1 \in [-2, 2]$. Aerodynamic data for a number of 438 configurations uniformly distributed in the parameter space was computed with VLM. It is normalised in a range of $[-1, 1]$ so that all inputs and outputs have the same order of magnitude and interpolation returns accurate results. In addition, only interpolation is allowed in order to avoid inaccuracy due to extrapolation.

The surrogate model based on RBF is described first. Its application is composed of three steps. First, an RBF function is chosen. Secondly, the RBF matrix is assembled, inverted and stored in memory. Thirdly, the interpolation is computed by exploiting the inverted matrix only when aerodynamic data is requested by the performance model. Concerning the radial basis function, it should be chosen according to the data to be interpolated and a brief investigation was performed. Three radial functions are compared in Fig. 10(a) for values of distance $\rho \in [0, \sqrt{7}]$. Note that the maximum distance ρ between any two configurations is $2\sqrt{7}$ because of the input data normalisation. The three functions assign different weights to configurations in the parameter space. Thin Plate Spline (TPS) function is defined as $\phi(\rho) = \rho^2 \log \rho$ and it assign a higher weight to configurations far in the parameter space. Conversely, Gaussian function $\phi(\rho) = e^{-\rho^2}$ relies on configurations closer than half parameter space. A modified version of the Gaussian, specifically $\phi(\rho) = 2^{-4\rho^2}$, is defined to assess RBF when configurations closer than a quarter of parameter space are considered. Performances of the three functions were compared by running a two-objective optimisation aiming to minimise both OEW and drag coefficient. Results are depicted in Fig. 10(b) where a comparison with VLM is included as well. Three approximations of the Pareto front were produced. Using the Gaussian function leads to results which reproduce the general trend with an average error of 10.0%. Results produced with the modified Gaussian function match accurately the reference for configurations located in the central region of the Pareto front and an average error of 11.5% is found. Conversely, TPS, which focus on far configurations instead, provides the best results in any region of the Pareto front with an average error of 7.62%.

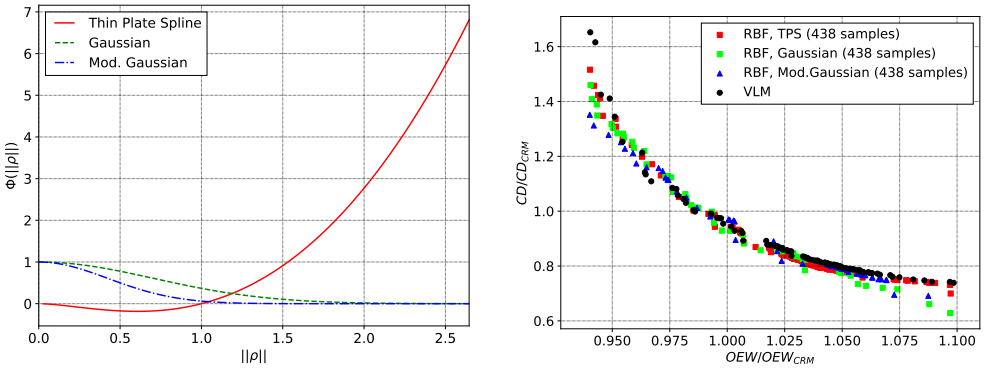

(a) RBF function (b) Pareto front

Figure 10. Multi-objective optimisation using RBF (438 pre-computed samples).

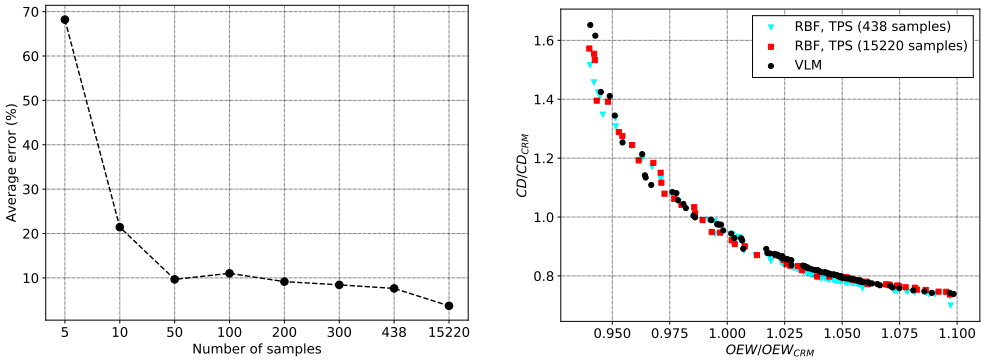

(a) Average error with respect to the number of samples using TPS.

(b) Pareto front produced with TPS using 438 and 15220 samples

Figure 11. Influence of the number of samples on the MDO results.

The trend was confirmed by running the same optimisation using RBF interpolation with a database containing 5, 10, 50, 100, 200, 300 samples. Although results are not reported here for sake of brevity, the TPS function consistently provided the least error. All databases with less than 400 configurations returned an error larger than 9% with respect to the VLM reference and the convergence curve is shown in Fig. 11(a). An additional simulation with a database build with 15220 configurations uniformly distributed in the parameter space was performed. Such large number of configurations is impractical for industrial application but it is useful for academic investigation. An average error of 3.70% is found when TPS is adopted whereas Gaussian and modified Gaussian functions provide an average error of 4.0% and 9.34%, respectively. In Fig. 11(b), Pareto fronts identified using TPS with 438 and 15220 samples are compared. Increasing the number of samples by a factor of 35 leads to better results since a difference of 3.92% between the two set of results is found. The TPS function using 438 samples is chosen as reference RBF model since it represents a trade-off between accuracy and number of samples.

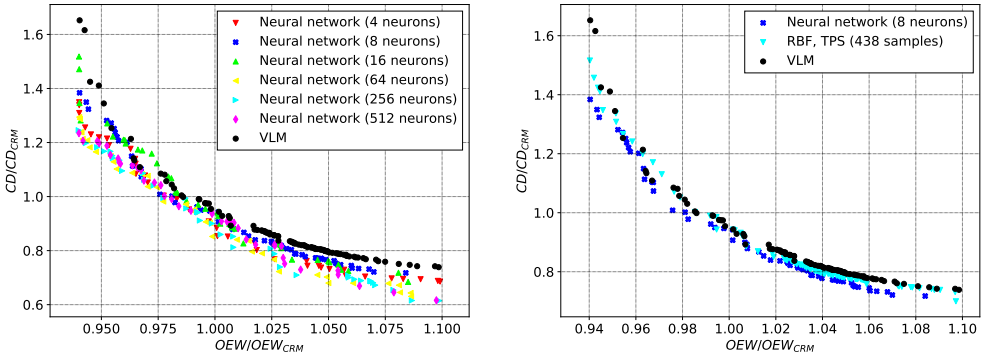

(a) Neural network performance

(b) Pareto front comparison

Figure 12. Comparison of multi-objective optimisation using RBF and Neural Network as surrogate models.

The surrogate model based on neural network is described next. Note the same database and the same scaling of input and output variables employed for the RBF model were used to train the neural network as well. A brief investigation was performed to choose the size of the network. Regarding inner and outer layers, the amount of neurons is defined by the number of inputs and outputs. According to the number of inputs (7) and outputs (8), guidelines proposed in [25] suggest a number of hidden neuron ranging from 7 to 20. Thus, three two-objective simulations aiming to minimise OEW and drag coefficient were performed with a size of the hidden layer ranging between 4 and 16. In addition, three large values (specifically 64, 256 and 512) were included in the investigation as well. Results are reported in Fig. 12(a) and they are compared to VLM reference. Using 4 neurons produces configurations which dominate the VLM ones. However, a quantification of the error showed that the neural network overestimated the performance and an average error of 10.4% was found. Increasing the number of neurons to 8 improves the results. Using neural networks, the smallest average error of 9.6% is found for 8 neurons. Further increasing their number to 16, 64, 256, 512 leads to inaccuracies and the average error becomes 11.2%, 12.7%, 11.2% and 14.6%, respectively. In Fig 12(b), a comparison of results produced with all models described so far is presented. Both surrogate models are able to identify the Pareto front accurately. However, the good agreement is limited to the central region of the Pareto front when it comes to neural network.

A summary concerning the computational cost of surrogate modelling is given. Statistics is reported here for the RBF model which uses TSP and the neural network with 8 neurons. Note that only the aerodynamic model is replaced and when evaluating the objective function, part of computational time is still employed to run the mass estimation model, stability model as well as to transfer data. Computations were performed using a single core of an Intel i7 4810MQ CPU. The total computational cost is split into two contributions. The first one is the computation of the aerodynamic database which was used by both surrogate models. It took 438 evaluations of the objective function using VLM for a total of 17 m 50 s which includes 1 s for each evaluation to execute all models and transfer the data. Regarding RBF, the matrix inversion needed to compute RBF coefficients took roughly 5 s and it was performed once. Secondly, interpolation of aerodynamic data for one configuration took 0.23 s and this task had to be repeated for 48 iteration and a swarm size of 128. Thus, the total time needed to run the MDO simulation with RBF model is 41m 20s split between

building the surrogate model (17 m 50 s) and using it (23 m 30 s). Regarding the surrogate model based on neural network, it needs 25 m 51 s to perform the optimisation for a total of 43m 41s, which is comparable to the amount of time needed by the RBF model. These numbers compare to the VLM reference. The cost of evaluating the objective function using aerodynamics based on VLM is 1.5 s on a Intel i7 4810MQ CPU and this task was repeated for 48 iteration and a swarm size of 128. The total time employed to perform the optimisation is about 2 h 33 m using a single core.

4.2 Hybrid modelling for aerodynamics

Although surrogate models proved to be a promising way to speed-up multidisciplinary optimisation, their bottleneck is collecting data for the training step. A solution is proposed by developing a hybrid model which can run either VLM or its surrogate according to the need. When aerodynamic data is requested, the surrogate model based on RBF is employed to compute an approximation. Quality of results is assessed using a criterion, which is discussed in the next paragraph, and two scenarios are then possible. If the criterion is satisfied, aerodynamic data is returned and no further action is taken. If not, a VLM simulation is performed and its results are returned as well as stored in a database to improve the surrogate model. Note that only VLM solutions populate the database for RBF model. At each iteration, RBF coefficients are computed by inverting the RBF matrix and stored for successive interpolations. Until the first iteration is complete, only VLM aerodynamics is adopted so that a database of aerodynamic data is available for RBF interpolation starting from the second iteration.

Regarding the criterion for switching between VLM and RBF, it is based on statistical analysis of previous optimisation data. Specifically, two set of results were considered. The first one is composed of all configurations assessed with VLM during the two-objective optimisation aiming to minimise OEW and drag coefficient. They were depicted in Fig. 7. The second one contains data produced with RBF model when performing the same optimisation. Results were already shown in Fig. 11(b). Each set is considered in turn. For each wing planform, a number of neighbouring configurations were identified based on their Euclidean distances in the parameter space. The standard deviation σ between aerodynamic data for the specific configuration (i.e. lift and drag coefficients, elevator deflection, angle of attack etc) and for its close neighbours was computed. As a result, a cumulative distribution which links σ to the percentage of configurations with a lower value of standard deviation is obtained. In Fig. 13(a), such distribution is shown for both databases and for three numbers of neighbours, specifically 2, 4 and 8. Values of σ ranging from 0 to 0.35 are found. Note that aerodynamic data for 95% of configurations has a standard deviation of less than $\sigma < 0.225$ when 2 or 4 neighbours are considered. A close-up in the region around $\sigma \approx 0.225$ is depicted in Fig. 13(b). It is shown that results produced with VLM and RBF converge to $\sigma \approx 0.25$ when the number of neighbouring configuration is 8. Information in Fig. 13 was exploited to set a threshold $\sigma_t = 0.15$ and a number $N = 5$ of neighbours as a criterion to switch between VLM and RBF model. Interpolated data is considered reliable when its standard deviation from the closest 5 neighbours σ is $\sigma < \sigma_t$.

Performing a two-objective optimisation to minimise OEW and drag coefficient with the hybrid model using a swarm size of 128 for 48 iterations, a threshold $\sigma_t = 0.15$ and a number $N = 5$ of neighbours took 44 m 17 s on a Intel i7 4810MQ CPU using a single core. Results are shown in Fig. 14. The ratio between the number of evaluations of the objective function using VLM and RBF is depicted in Fig. 14(a). The first iteration is performed with

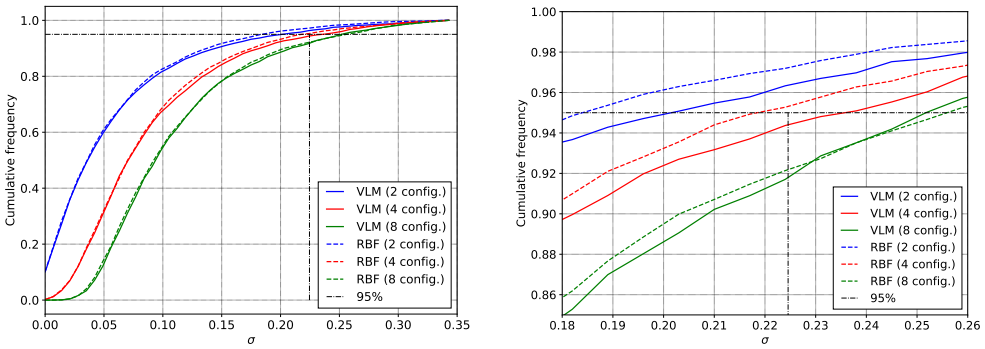

(a) Global distribution (b) Close up

Figure 13. Cumulative distribution of standard deviation used to identify the threshold value for the hybrid aerodynamic model.

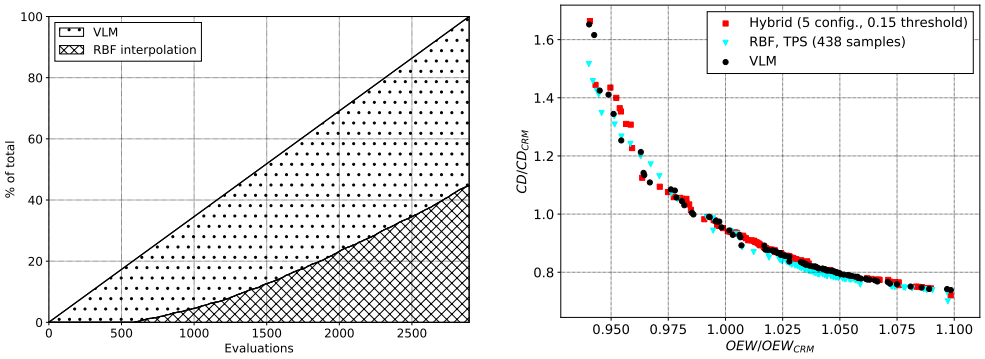

(a) Type of simulation (b) Pareto front

Figure 14. Multi-objective optimisation using the hybrid model. Results are compared to VLM as well as RBF.

VLM since no database is available to perform RBF interpolation. The following 3 iterations show no contribution by the surrogate model as well. This is due to values of σ for interpolated aerodynamic data which are above the threshold $\sigma_t = 0.15$. Starting from the fifth iteration, results from the surrogate model are considered accurate with $\sigma < \sigma_t$. The number of evaluations performed with RBF increases and by the end of the simulation a total of 43% of configurations was assessed exclusively with the surrogate model. The Pareto front obtained with the hybrid model is compared to the ones computed with RBF and VLM in Fig. 14(b). Overall, a very good agreement is found between the hybrid model and the VLM reference. Results for the lower region of the Pareto front match accurately and the upper region, for which fewer configurations are available, is identified too. In addition, a comparison is provided between the hybrid model and the RBF one. The latter is able to reproduce the upper region of the Pareto front properly. Concerning the lower part, the hybrid model provides more accurate results.

Method	Average error	Standard deviation	Computational time
VLM	-	-	100%
RBF	7.62%	14.6%	27.0%
Neural Network	9.60%	17.0%	28.5%
Hybrid	0.784%	2.32%	28.9%

Table 2. Performance of surrogate models for aerodynamics. Error and its standard deviation are referred to the exact value computed with VLM and expressed as a percentage.

A quantitative summary of the investigation concerning surrogate modelling for aerodynamics using RBF, neural network and hybrid model is provided in Table 2. Results for the same two-objective optimisation aiming to minimise OEW and drag coefficient are compared. The surrogate model based on RBF interpolation identifies the Pareto front with an average error of 7.62%. The computational cost is reduced to almost a quarter of the VLM and this figure is similar for all surrogate models. The neural network is the least performing of the surrogate models since its error is 11.2% on average and the corresponding computational time is decreased to 28.5%. Conversely, the hybrid model provides the best results with an error smaller than 1% at the same computational cost. The total time needed by the hybrid optimisation is 44m 17s since evaluations took 1.5s and 0.23s using VLM and RBF, respectively. A higher number of VLM evaluations (around 1500) is performed for the hybrid model when compared to the RBF surrogate, which used 438 VLM simulations for the sampling instead. However, the computational time for data-transferring and execution of external models is negligible for the hybrid optimisation since both VLM and RBF are now part of the same model and no additional overheads is needed. Note also that the computational time and accuracy of the hybrid model changes as a function of the threshold. For example, further reduction of time were obtained by performing the same two-objective optimisation using a threshold $\sigma_t = 0.20$. An average error of 1.18% was found and the total computational time was 27 m 41 s which is 18% of the reference.

5.0 Conclusions and next steps

The development of a novel model-based framework for multidisciplinary wing planform optimisation at early-stage aircraft design is presented in this paper. The software is composed of a particle swarm optimiser and a performance model for the assessment of new planform configurations. The latter consists of multiple interacting models which focus on distinct disciplines such as aerodynamics, mass estimation and longitudinal stability.

An application of the framework to optimise the wing planform of the Common Research Model is presented. Results are discussed for single-objective, two-objective and multi-objective optimisations using vortex lattice aerodynamics. Some optimal configurations located on Pareto fronts are analysed in detail. Overall the framework provides effective guidance to the human designer who receives suggestions on modifications which improve the reference geometry.

The modal-based framework allows the substitution of models at any time. This feature was exploited to investigate on surrogate modelling for aerodynamics at early-stage design. A key challenge is to cope with a large variety of wing planforms and two methods were assessed using the same training data. First a surrogate model based on Radial Basis Function

interpolation is presented. Secondly, a neural network with three layers is described. The former provides accurate results and a reduction of about 75% in terms of computational cost. The main limitation of surrogate models is the need for a training set of data. This problem was addressed developing a hybrid model which switches automatically between vortex lattice aerodynamics and the surrogate model. The switching criterion is defined in an objective way to rule out any arbitrariness. Overall, the hybrid model provides excellent accuracy at the computational cost of surrogate models.

Future work will focus on developing a new aerodynamic model based on a high-fidelity tool such as computational fluid dynamics. In addition, the mass estimation model will use in-house tools based on experimental data.

Acknowledgements

Authors want to acknowledge the support received from Airbus UK, in particular from the Future Project Office. The research is part of the Agile Wing Integration programme sponsored by Innovate UK.

REFERENCES

1 . J. Slotnick, A. Khodadoust, J. Alonso, D. Darmofal, W. Gropp, E. Lurie, and D. Mavriplis. CFD vision 2030 study: a path to revolutionary computational aerosciences. Technical report, NASA Langley Research Center, 2013.

2 . T. Pardessus. Concurrent engineering development and practices for aircraft design at Airbus. In *24th Congress of International Council of the Aeronautical Sciences*, Yokohama, Japan, August 2004.

3 . C. Audet and M. Kokkolaras. Blackbox and derivative-free optimization: theory, algorithms and applications. *Optimization and Engineering*, 17(1):1–2, Mar 2016.

4 . D. P. Raymer. *Enhancing aircraft conceptual design using multidisciplinary optimization*. Kungliga Tekniska högskolan, Institutionen för flygteknik, 2002.

5 . J. Demange, M. A. Savill, and T. Kipouros. Multifidelity optimization for high-lift airfoils. In *54th AIAA Aerospace Sciences Meeting*, San Diego, California, January 2016.

6 . S. Kontogiannis, M. A. Savill, and T. Kipouros. A multi-objective multi-fidelity framework for global optimization. In *58th AIAA/ASCE/AHS/ASC Structures, Structural Dynamics, and Materials Conference*, Grapevine, Texas, January 2017.

7 . G. Ferraro, T. Kipouros, M. A. Savill, and A. Rampurawala. Multi-objective genetic design optimisation for early design. In *52nd Aerospace Sciences Meeting, AIAA SciTech Forum*, National Harbor, Maryland, January 2014.

8 . J. Martins and A. Lambe. Multidisciplinary design optimization: a survey of architectures. *AIAA Journal*, 51:2049–2075, 2013.

9 . J. Yoon, N. V. Nguyen, S. Choi, J. W. Lee, S. Kim, and Y. H. Byun. Multidisciplinary general aviation aircraft design optimizations incorporating airworthiness constraints. In *10th AIAA Aviation Technology, Integration, and Operations (ATIO)*, Fort Worth, Texas, September 2010.

10. I. Lind and H. Andersson. Model based systems engineering for aircraft systems - how does Modelica-based tools fit? In *8th International Modelica Conference*, Dresden, Germany, March 2011.

11. J. A. Estefan. Survey of model-based systems engineering (MBSE) methodologies. *Incose MBSE Focus Group*, 25(8):1–12, 2007.

12. D. J. Armstrong. The quarks of object-oriented development. *Communications of the ACM*, 49(2):123–128, 2006.

13. M. Reyes-Sierra and C. A. Coello. Multi-objective particle swarm optimizers: a survey of the state-of-the-art. *International Journal of Computational Intelligence Research*, 2(3):287–308, 2006.
14. E. Torenbeek. *Advanced aircraft design: Conceptual design, technology and optimization of subsonic civil airplanes*. John Wiley & Sons, 2013.
15. R. Bisplinghoff, H. Ashley, and R. Halfman. *Aeroelasticity*. Addison-Wesley, 1955.
16. J. Katz and A. Plotkin. *Low-Speed Aerodynamics*. Cambridge Aerospace Series. Cambridge University Press, 2nd edition, 2001.
17. M. Drela and H. Youngren. AVL-aerodynamic analysis, trim calculation, dynamic stability analysis, aircraft configuration development. *Athena Vortex Lattice*, 3:26, 2006.
18. M. D. Buhmann. *Radial Basis Functions: Theory and Implementations*. Cambridge University Press, 2003.
19. H. Wendland. *Scattered Data Approximation*. Cambridge Monographs on Applied and Computational Mathematics. Cambridge University Press, 2004.
20. M. van Gerven and S. Bohte. Artificial neural networks as models of neural information processing. *Frontiers in Computational Neuroscience*, 11(114):1–2, 2017.
21. D. W. Ruck, S. K. Rogers, M. Kabrisky, M. E. Oxley, and B. W. Suter. The multilayer perceptron as an approximation to a bayes optimal discriminant function. *IEEE Transactions on Neural Networks*, 1(4):296–298, 1990.
22. D. E. Rumelhart, G. E. Hintont, and R. J. Williams. Learning representations by back-propagating errors. *Nature*, 323(6088):533–536, 1986.
23. F. Pedregosa, G. Varoquaux, A. Gramfort, V. Michel, B. Thirion, O. Grisel, M. Blondel, P. Prettenhofer, R. Weiss, V. Dubourg, J. Vanderplas, A. Passos, D. Cournapeau, M. Brucher, M. Perrot, and E. Duchesnay. Scikit-learn: Machine learning in Python. *Journal of Machine Learning Research*, 12:2825–2830, 2011.
24. J. Vassberg, M. A. Dehaan, M. Rivers, and R. Wahls. Development of a common research model for applied CFD validation studies. In *26th AIAA Applied Aerodynamics Conference*, Honolulu, Hawaii, August 2008.
25. J. Heaton. *Introduction to Neural Networks for Java*. Heaton Research, Inc., 2nd edition, 2008.